

Nature of Correlated Motion of Electrons in the Parent Cobaltate Superconductors

M.Z. Hasan,^{1,*} D. Qian,¹ Y. Li,¹ A.V. Fedorov,² Y.-D. Chuang,² A.P. Kuprin,² M.L. Foo,³ and R.J. Cava³

¹*Department of Physics, Joseph Henry Laboratories, Princeton University, Princeton, NJ 08544*

²*Advanced Light Source, Lawrence Berkeley National Laboratory, Berkeley, Ca 94305*

³*Department of Chemistry, Princeton University, Princeton, NJ 08544*

(Dated: October 5, 2018)

Recently discovered class of cobaltate superconductors ($\text{Na}_{0.3}\text{CoO}_2 \cdot n\text{H}_2\text{O}$) is a novel realization of interacting quantum electron systems in a triangular network with low-energy degrees of freedom. We employ angle-resolved photoemission spectroscopy to uncover the nature of microscopic electron motion in the parent superconductors for the first time. Results reveal a large hole-like Fermi surface (consistent with Luttinger theorem) generated by the crossing of super-heavy quasiparticles. The measured quasiparticle parameters collectively suggest a two orders of magnitude departure from the conventional Bardeen-Cooper-Schrieffer electron dynamics paradigm and unveils cobaltates as a rather hidden class of relatively high temperature superconductors.

PACS numbers: 71.20.b, 73.20.At, 74.70.b, 74.90.+n

Research on strongly correlated electron systems has led to the discovery of many unconventional states of matter as such realized in the high temperature superconductors, quantum Hall systems or in the charge-orbital ordering magnetic compounds. Recently, attention has focused on layered cobalt oxides $\text{Na}_x\text{CoO}_2 \cdot n\text{H}_2\text{O}$ - a new class of doped Mott insulator which in addition to being strongly correlated are also frustrated in their magnetic interactions. Depending on the carrier concentrations, cobaltates exhibit colossal thermoelectric power, dome-shaped superconductivity and charge-density-wave phenomena[1]-[5]. They carry certain similarities such as the two dimensional character of non-Fermi-liquid electron transport, spin-1/2 magnetism and dome-shaped superconductivity as observed in the cuprate superconductors[1]-[7]. Unlike cuprates, cobaltates can be carrier doped over a much wider range and allow to study emergent behavior in a very heavily doped Mott insulator. Previous ARPES studies have focused on the high doping regime ($x=70\%$, TE-doping) where colossal thermopower is observed [8]. Transport, magnetic and thermodynamics measurements suggest that the electron behavior is dramatically different in low sodium doping ($x=30\%$, SC-doping) where superconductivity is observed [5, 9]. We have carried out (for the first time) a detailed microscopic study of the single electron motion in the parent cobaltate superconductor (low doping regime) class which reveals the novel many-body state of matter realized in this system.

Spectroscopic measurements were performed at the Advanced Light Source. Most of the data were collected with 90 eV or 30 eV photons with better than 30 or 15 meV energy resolution, and an angular resolution better than 1% of the Brillouin zone at ALS Beamlines 12.0.1 and 7.0.1 using Scienta analyzers with chamber pressure better than 8×10^{-11} torr. A key aspect of the success of our spectroscopic studies has been a careful growth and characterization of high quality single crystals and

precise control of sodium concentration[2, 5]. Cleaving the samples in situ at 20 K (or 100K) resulted in shiny flat surfaces, characterized by diffraction methods to be clean and well ordered with the same symmetry as the bulk. No Ruthenate-like surface state behavior was observed in high quality samples and all the data taken at 20K although cleaved at 100K in a few cases for careful cross-checking.

Fig-1(a-d) shows representative single electron removal spectra as a function of energy and momentum in $\text{Na}_{0.3}\text{CoO}_2$. A broad quasiparticle (electron dressed with interactions) feature is seen to disperse from high binding energies at high momentum values near the corner (K) or the face (M) of the crystal reciprocal space (Brillouin zone, BZ) to the Fermi level (zero binding energy). This electron-feature grows in intensity (yellow emerging from red) before crossing the Fermi level. This is the quasiparticle band in this system. It is a hole-like[8, 9] band since the bottom of the band is located near the zone boundary (K or M) as opposed to the zone center. We trace the momentum values (k) of the electron (quasiparticle)'s zero-binding energy crossing point over a large part of the Brillouin zone. This allows us to generate a momentum space density of states "n(k)" plot (Fig.2(a)). The inner edge of this density plot is the Fermi surface. It is a large rounded hole around the zone center. The Fermi surface of the parent superconductor ($x=30\%$, SC-doping) as we report here exhibits more hexagonal character than the related thermoelectric compound ($x=70-75\%$, TE-doping)[8]. This shape is similar to the Local Density Approximation calculation[10]. However, no satellite pocket is observed. This could be due to strong correlation effects, which can push the minority bands away from the Fermi level deep below in binding energies and wash out their relative intensity. A large Hubbard-U (~ 4 eV) can be extracted by fitting the valence excitations with a cluster model [8]. The size of the Fermi surface, $k_f \sim 0.8 \text{ \AA}^{-1}$, for the SC-doping studied here is larger

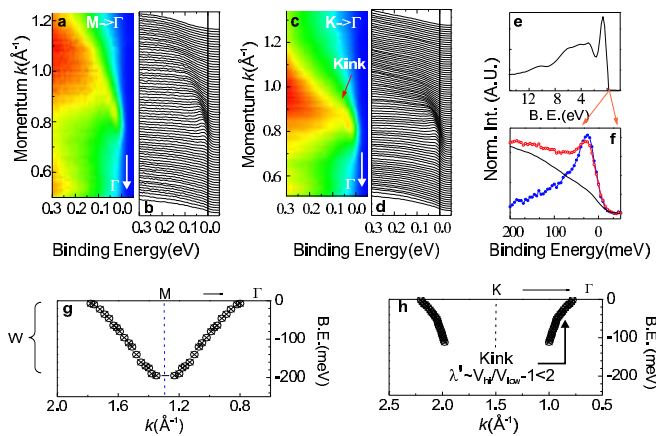


FIG. 1: **Single-Particle Dispersion:** Zone face to the zone center ($M \rightarrow \Gamma$): a, Spectral intensity. b, Energy dispersion curves; Zone corner to the zone center ($K \rightarrow \Gamma$): c, Spectral intensity. d, Energy dispersion curves. Color red/blue corresponds to high/low intensity. e, Valence band. f, Quasiparticles. g, Dispersion relation, E vs. k along $M \rightarrow \Gamma$ (extracted after background correction and symmetrized around the M point). The bandwidth (W) ~ 200 meV is estimated by tracing/extrapolating the band to the zone boundary shown in (g). h, The raw dispersion (background not subtracted) along the $K \rightarrow \Gamma$ cut shows a kink (also seen in the raw data (c)). All the data were taken at 20K.

than the size observed in the TE-doping[8] suggesting a hole doping picture of these compounds (since $x=30\%$ samples have more holes)(Fig.2(b)). The Fermi surface area suggests that about 64% of the Brillouin Zone is electron-occupied. This is consistent with the conventional electron count in the $x=30\%$ compound. Hence Luttinger theorem is satisfied in a conventional sense. For the SC-doping, the carrier sign of thermopower or Hall transport[4, 5] being positive at all temperatures suggests that it is the holes that carry the current - a fact consistent with our finding of a hole-like Fermi surface.

In order to estimate the total bandwidth we need to obtain the complete dispersion relation (energy vs. momentum) over the full Brillouin zone. To achieve this we extrapolate the quasiparticle band to the zone boundary (Fig.1(g)). This gives a value of the total energy dispersion, or bandwidth, of about $180 \text{ meV} \pm 20 \text{ meV}$ ($\sim 0.2 \text{ eV}$). This bandwidth is about a factor of two larger than the bandwidth observed in the thermoelectric (TE-doping, $x \sim 70\%$) cobaltates[8] suggesting a more delocalization (electron-wavefunctions spread out more) of carriers in the parent superconductor. Larger bandwidth may be responsible for weaker thermopower observed near superconducting doping because within a Fermi liquid picture thermopower is inversely related to the bandwidth[3, 9]. However, the observed bandwidth is still much smaller than the value calculated ($\sim 1.5 \text{ eV}$) using the Local Density Approximation methods[10]

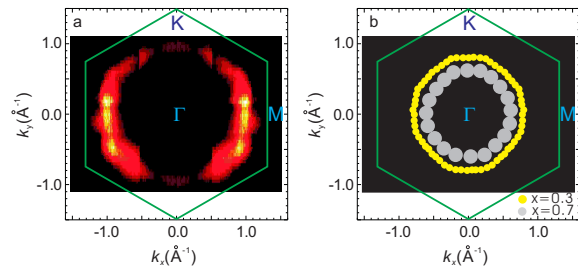


FIG. 2: **Fermi Surface of Parent Superconductor:** a, Momentum-space density of states ($n(k)$) plot shows a large hole-pocket centered around the Γ -point. The inner edge of the pocket is the Fermi surface which exhibits some hexagonal anisotropy. b, Comparison of the Fermi surface between parent superconductor ($x=0.3$) and the thermoelectric ($x=0.7$) host compound.

which does not consider electron correlation effects. The bandwidth measured here is consistent with that extracted/estimated from the bulk thermal measurements on the hydrated superconducting samples[7]. The specific dispersion behavior (band having maximum at the zone boundary or emanating from the zone boundary to cross Fermi level in moving towards the zone center) indicates a negative sign [12]-[14] of effective single-particle hopping ($t < 0$). This sign is crucial in describing the physics in a triangular network. The possibility of superconductivity and its doping dependence in triangular many-body models such as Hubbard model or t - J model crucially depend on the sign of t [12]-[15]. Hence, our unambiguous determination of a negative sign of t in the SC-doping compound has implications for the possibilities of superconducting order parameters (such as $d_{x^2-y^2}$) it can sustain: $d_{x^2-y^2}$ superconductivity is fragile for a negative t model whereas it is robust for positive t . Furthermore, a negative t rules out the possibility of Nagaoka-type ferromagnetic instability[13] in these systems. However, next neighbor Coulomb interaction can stabilize superconductivity in the presence of a negative t and restore Resonating Valence Bond mechanism of superconductivity[15].

We then estimate an effective Fermi velocity, which is roughly the slope of the dispersion relation or the derivative of the band[9] evaluated very close to the Fermi level, by analyzing the dispersion curves in Fig.1(a-d). The Fermi velocity, averaged over the entire Fermi surface is found to be about $0.15 \pm 0.05 \text{ eV}\cdot\text{\AA}$ (about $0.2 \text{ eV}\cdot\text{\AA}$). This is quite small compared to most known correlated layered oxides. The velocity is about a factor of 10 smaller than the superconducting cuprates[16]. Given the size of the Fermi surface we estimate the carrier mass, $m^* \sim \hbar k_f / |v_f| \sim 60 m_e$. This is a rather large carrier mass for a high-conductivity transition metal oxide. Similarly large carrier mass has recently been reported by

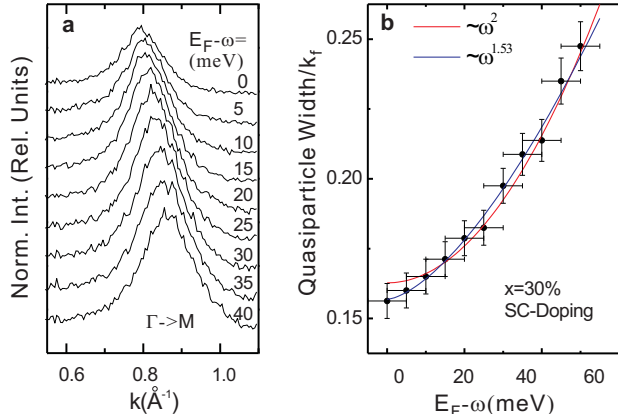


FIG. 3: **Self-energy Behavior:** a, Momentum distribution curves along $M \rightarrow \Gamma$ shows changes of lineshapes away from the Fermi level (0 meV). b, Quasiparticle (lineshape) width in $x=30\%$ sample (superconducting doping) plotted as a function of binding energy, which shows nearly ω^2 (quadratic) Fermi-liquid-like behavior.

muon spin rotation measurements[18]. Such large carrier masses are typically seen in the heavy-fermion compounds ($\sim 100 m_e$), where the low-energy physics arises from two hybridized bands including an atomic-like f -electron band, but are rarely observed in the transition metal oxides. How cobaltates exhibit such a large carrier mass where only a single d -band is at play remains to be understood.

We further observe that electron velocity changes beyond 50-70 meV binding energy range and a kink (Fig.1(c)) is observed in the dispersion relation along the $\Gamma \rightarrow K$ direction in that energy range. This could be due to coupling to bosonic collective modes such as phonons or magnetic fluctuations (kink in Fig.1(c) and 1(g)). The energy scale of the kink - the velocity cross-over - directly corresponds to the optical phonon (Raman-active lattice vibrations 55-75 meV) energies in the cobaltates [19]. Based on the kink parameters (ratio of high-energy velocity and low-energy velocity) in our data the effective coupling is on the order of unity which is very similar to what is observed in the cuprates[16]. A similar kink was also reported in the high doping regime [8]. Its observation indicates the existence of strong bosonic interaction or coupling in the single-particle dynamics of the cobaltates. It would be interesting to look for such modes using inelastic x-ray [20] or neutron scattering.

We study the scaling behavior of the electron self-energy based on the momentum distribution curves shown in Fig.3(a). The quasiparticle line widths which provide a measure of electron self-energy or scattering rate, as a function of electron binding energy (ω) can be fitted with a quadratic-like ($\omega \sim 2$) form (Fig.3(b)) with a large prefactor than conventional metals [9, 11]. This

suggests that the system can be thought of as a strongly renormalized heavy-Fermi liquid. This scaling behavior is in significant contrast with our findings in the thermoelectric cobaltates ($x=70\%$) [8].

To gain further insights into the nature of electron motion, we now compare the basic electronic parameters of the cobaltates with other classes of layered oxide superconductors and conventional BCS superconductors (Table 1). Based on our finding of electron behavior, we note that the cobaltates have a large on-site electron-electron interaction energy (U , measured in a similar manner described in Ref. [8]) comparable to the superconducting cuprate family[16] but both the bandwidth and the Fermi velocity are several fold smaller and the nodal carrier mass is orders of magnitude larger (Table 1). To compare superconducting properties, we define a parameter $k_B T_c^{max}/W$ which compares two *fundamental* energy scales in an electronic system. The quantity $k_B T_c$ (T_c is the transition temperature and k_B is the thermal Boltzmann constant) describes the superconducting condensation temperature/energy scale and W is the total effective bandwidth that describes the total kinetic energy available to the electron system. We make a plot, shown in Fig.4(A), of the quantity, transition temperature as a fraction of quasiparticle bandwidth, $k_B T_c^{max}/W_{ARPES}$ (maximum transition temperature is considered in doped systems) for several major classes of layered (quasi-2-D materials) superconductors[16, 17]. We then locate the cobaltate class based on our data. It is evident from Fig.-4(a) that the ratio, $k_B T_c^{max}/W_{ARPES}$ ($\sim k_B * 5 \text{ Kelvin} / 0.2 \text{ eV} \cdot \text{\AA} \sim 0.002$) for the cobaltate system is about two orders of magnitude larger than the strong coupling BCS superconductors such as tin (Sn) or lead (Pb)[21]. The cobaltate value is rather close to that observed in the cuprate superconductors or doped fullerenes[22] where both strong electron-electron and electron-boson (or phonon) interactions are observed. A two-orders-of-magnitude departure from the conventional phonon-only BCS-like value in the cobaltates is a signature for its electron dynamics to be of unconventional origin in the sense that phonons alone can not be accounted for superconductivity. Electron-electron interaction leads to a reduction or renormalization of W which is a manifestation of the strong correlation (Mott) effect. This strong electron-electron (Mott effect) interaction leads to the enhancement of the quantity T_c/W . In order to further test its relevance to superconductivity in the sense that T_c/W reflects a measure of relative effective interaction strength (from one class to the other) we plot this quantity against a known independently measured parameter - the inverse coherence length ($1/\xi$) which is an inverse measure of the size of the superconducting electron-pair wavefunction hence a measure of the overall coupling strength (interactions) from one materials class to the other. In Fig-4(b) we plot T_c^{max}/W_{ARPES} vs. ξ^{-1} and observe that this is true for most classes

TABLE I: ARPES Quasiparticle parameters for major classes of superconductors

Class	T_c (K)	Bandwidth W_{APRES} (eV)	Fermi velocity $v_{f[ARPES]}$ (eV·Å)	Mass m/m_e	Hubbard U (eV)	Ref.
Cobaltates(NaCoO)	5	0.18±0.04	0.15±0.10	60±20	>4.0	Present work
p-Cuprates(LSCO)	38	~0.4	1.8	2 (nodal)	3 - 5	[16]
n-Cuprates(NCCO)	22	~0.5	2.0	2.4 (nodal)	~3	[17]
Ruthanates(SrRuO)	1	0.5	0.4 (avg)	~9 (avg)	1	[16]
BCS-type SCs(Pb)	7.2	9.5	12	2		[21]

of modern (unconventional) superconductors as well as for the BCS superconductors suggesting a universal behaviour. Given the slope of the line (~ 0.02 nm) and our T_c/W (~ 0.002) data on cobaltates measured here, we make an empirical estimate of $1/\xi$ for the cobaltates which is found to be about $(0.002/0.02 \text{ nm} \sim 0.1)$ inverse nanometer. This agrees remarkably with recent estimates of coherence length based on magnetic field measurements within the same order-of-magnitude[6, 7]. We further plot dc conductivity[5, 16, 22, 23] as a function of quasiparticle bandwidth in conventional and unconventional superconducting materials, which suggests that cobaltates (Fig.-4(c)) fall closer to the cuprates or ruthanates but in a different regime where magnesium diboride belongs to.

The fact that the cobaltate system has a relatively large transition temperature as a fraction of quasiparticle bandwidth and small Fermi velocity is rather remarkable. This suggests that given the total bandwidth or total kinetic energy, the system has achieved superconductivity at a relatively high temperature although the actual T_c is rather low in absolute numbers. In this sense it is a hidden "high temperature superconductor" even though it may have a very different order parameter symmetry than the cuprates.

Our results provide the fundamental electron parameters (Fermi surface topology, sign of hopping, Fermi velocity, quasiparticle mass, bandwidth etc.) to construct a model hamiltonian for the cobaltate class. The unusual character of the microscopic electron dynamics in the cobaltates observed here suggests that any comprehensive theory of these materials needs to account for the fact that a relatively large value of transition temperature is achieved in an extremely narrow band parent material with unusually heavy and slow moving carriers where a two-orders-of-magnitude departure from conventional phonon-only BCS paradigm is observed in the microscopic electron dynamics. The observed electron dynamics of the cobaltates also point to an emergent unifying theme in the intrinsic physics of modern unconventional superconducting materials.

We gratefully acknowledge N.P. Ong, P.W. Anderson, G. Baskaran, P.A. Lee, S. Shastry, S. Sondhi and Z. Husain for valuable discussion. Experimental data were

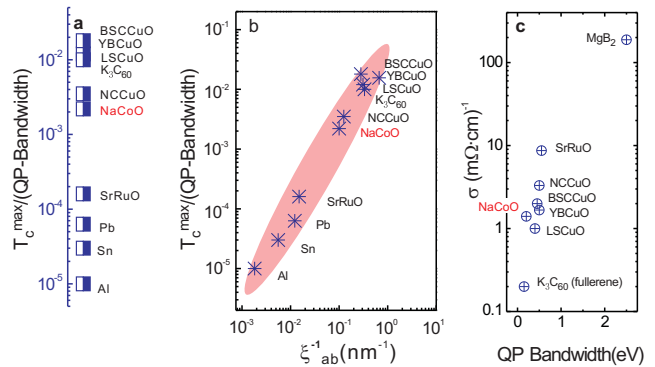


FIG. 4: **Quasiparticle-Bandwidth and Superconductivity:** a, Transition temperature (T_c) as a fraction of bandwidth ($T_c^{max}/\text{bandwidth}$) for several classes of superconductors. b, $T_c/(\text{ARPES-bandwidth})$ is found to scale with the inverse ab -plane coherence length. Coherence length data is taken from Ref. [24]. c, Electrical (dc) conductivity is plotted as a function of (ARPES) bandwidth for conventional and unconventional superconductor classes. In general, cobaltate class is found to cluster with the unconventional superconductors than the BCS type conventional superconductors. A characteristic two-orders-of-magnitude departure from conventional BCS-like behavior is evident in (a), (b) and (c).

recorded at ALS which is operated by the DOE Office of Basic Energy Science. MZH acknowledges partial support through NSF-MRSEC (DMR-0213706) grant. Materials synthesis and ARPES characterization was supported by DMR-0213706 and the DOE, grant DE-FG02-98-ER45706.

* To whom correspondence should be addressed: mzhasan@Princeton.edu

- [1] K. Takada *et al.*, Nature **422**, 53 (2003).
- [2] R. E. Schaak *et al.*, Nature **424**, 527 (2003).
- [3] I. Terasaki, Y. Sasago, K. Uchinokura, Phys. Rev. B **56**, R12685 (1997).
- [4] Y. Wang, N. S. Rogado, R. J. Cava, N. P. Ong, Nature **423**, 425 (2003).
- [5] M. L. Foo *et al.*, Phys. Rev. Lett. **92**, 247001 (2004).
- [6] H. Sakurai *et al.*, Phys. Rev. B **68**, 132507 (2004).

- [7] F. C. Chou *et al.*, Phys. Rev. Lett. **92**, 157004 (2004); R. Jin *et al.*, Phys. Rev. Lett. **91**, 217001 (2003)
- [8] M. Z. Hasan *et al.*, Phys. Rev. Lett. **92**, 246402 (2004). cond-mat/0308438 (2003).
- [9] C. Kittel, Introduction to Solid State Physics (Wiley, New York 5th Ed., 1976).
- [10] D. J. Singh, Phys. Rev. B **61**, 13397 (2000).
- [11] D. Pines, The Theory of Quantum Liquids (Adv. Book Classics Benjamin, NY, 1989).
- [12] G. Baskaran, Phys. Rev. Lett. **91**, 097003 (2003).
- [13] B. Kumar, B. S. Shastry, Phys. Rev. B **68**, 104508 (2003).
- [14] Q. -H. Wang, D. -H. Lee, P. A. Lee, Phys. Rev. B **69**, 092504 (2003).
- [15] O. I. Motrunich, P. A. Lee, Phys. Rev. B **69**, 214516 (2004).
- [16] A. Damascelli, Z. Hussain, Z. -X. Shen, Rev. Mod. Phys. **75**, 473 (2003).
- [17] N. Armitage *et al.*, Phys. Rev. Lett. **88**, 257001 (2002).
- [18] A. Kanigel *et al.*, Phys. Rev. Lett. **92**, 257007 (2004).
- [19] M. N. Iliev *et al.*, Physica C **402**, 239(2004).
- [20] M. Z. Hasan *et al.*, Phys. Rev. Lett. **88**, 177403 (2002). cond-mat/0406654 (2004).
- [21] C. P. Poole *et al.*, Superconductivity (Academic Press, San Diego, USA, 1995).
- [22] O. Gunnarsson, Rev. Mod. Phys. **69**, 575 (1997).
- [23] O. Klein *et al.*, Phys. Rev. B **46**, 11247(1992); B. J. Batlogg, Low Temp. Phys **95**, 23 (1994). J. M. Rowell, Supercond. Sci. Technol. **16**, R17 (2003).
- [24] Y. Wang *et al.*, Science **299**, 86 (2003).